Final state interaction observed in $M_{2,3}VV$ Auger profile of Cu(110)

2009 J. Phys.: Condens. Matter 21 055007

(http://iopscience.iop.org/0953-8984/21/5/055007)

J. Phys.: Condens. Matter **21** (2009) 055007 (5pp) doi:10.1088/0953-8984/21/5/055007

Final state interaction observed in $M_{2,3}VV$ Auger profile of Cu(110)

H Nakajima[1], M Buddhakala[2], S Chumpolkulwong[3], P Songsiriritthigul[1,4] and A Kakizaki[5]

[1] Synchrotron Light Research Institute, 111 University Avenue, Muang District, Nakhon Ratchasima 30000, Thailand
[2] Department of Physics, Faculty of Science and Technology, Rajamangala University of Technology Thanyaburi, 39 Muh 1, Rangsit-Nakhonnayok Road Klong Hok, Thanyaburi District, Pathumthani 12110, Thailand
[3] Department of Physics, Faculty of Science, Udon Thani Rajabhat University, 64 Thahan Road, Muang District, Udon Thani 41000, Thailand
[4] School of Physics, Suranaree University of Technology, 111 University Avenue, Muang District, Nakhon Ratchasima 30000, Thailand
[5] Institute for Solid State Physics, The University of Tokyo, Kashiwa, Chiba 277-8581, Japan

E-mail: hiden@nsrc.or.th

Received 25 September 2008, in final form 24 November 2008
Published 16 December 2008
Online at stacks.iop.org/JPhysCM/21/055007

Abstract
We have measured the $M_{2,3}VV$ Auger spectra of Cu(110) and studied the final state interaction following the Cu 3p core electron excitation. We have observed that the kinetic energy of the $M_{2,3}VV$ Auger electron shifts to an energy higher than that of the normal Auger electrons near the Cu 3p threshold, and it converges to the constant kinetic energy of the normal Auger electrons as the excitation energy increases above the Cu 3p threshold. In the excitation energy dependence of the kinetic energies of the $M_{2,3}VV$ Auger electrons, we observed step features at the excitation energies corresponding to the 3p core electron excitations to the L_1 and X_1 van Hove singularities in the valence states. The kinetic energy shifts of the $M_{2,3}VV$ Auger electrons are reasonably understood by considering the localization of the two-hole Auger final state and the hybridization between Cu 3d states and other valence states.

1. Introduction

Core level photoemission spectroscopy has been a crucial probe in studying the many-body interactions in the electron systems of solids [1–5]. The core level photoemission spectra often show multiplet and/or satellite structures, which originate from the large intra-atomic Coulomb interaction between a photoexcited core hole and the valence electrons as well as inter-atomic hybridization. In many cases, the photoexcited core hole decays via a non-radiative Auger process, and their spectral profiles show that the excitation energy dependence is associated with the characteristics of the valence structure and the details of the decay dynamics [6, 7]. It is known that in the valence band spectra of Ni metal the valence band satellite reveals resonant enhancement at the 3p core electron excitation threshold [8], which is understood as a result of the interference effect between the direct 3d valence electron excitation and the 3p core electron excitation followed by $M_{2,3}VV$ Auger decay, forming two 3d holes in a Ni atom [4].

Previously, Tanaka *et al* [9] studied the resonant behavior of Ni 3p and 3s satellites and the $L_{2,3}VV$ Auger profiles of molecular crystal $K_2Ni(CN)_4$ and Ni metal near the 2p core electron excitation threshold. They found that in $K_2Ni(CN)_4$ the kinetic energies of the $L_{2,3}VV$ Auger electrons decrease with an increase in excitation energy above the Ni 2p core electron excitation threshold. They implied that the strong localization of the two-hole final state in the molecular crystal causes the shift of the kinetic energies of the Auger electrons. They also showed that in Ni metal the kinetic energies of the $L_{2,3}VV$ Auger electrons reveal the same energies as those of the normal Auger electrons near the 2p core electron excitation threshold, since the two-hole final state is well screened by the conduction electrons. Recently, Föhlisch *et al* [10] measured the $L_{2,3}VV$ Auger spectra of Cu metal

by high energy resolution x-ray photoemission and found that the peak positions of the $L_{2,3}VV$ Auger profile are shifted from the constant kinetic energies near the Cu 2p core electron excitation threshold. They observed that the kinetic energies of the Auger electrons decrease near the excitation energies corresponding to the 2p core electron excitation to the L_1 and X_1 van Hove singularities in the valence states, which exist 4.2 and 7.7 eV above the Fermi level (E_F), respectively. They suggested that the observed shift depends on the core hole lifetime and that the shorter lifetime results in the larger peak shift. Hence, in the $L_{2,3}VV$ Auger process, the kinetic energy shift of the L_2VV Auger electrons is larger than that of the L_3VV Auger electrons [10, 11]. They also showed that the shift could be described by a numerical model of the resonant Auger theory, which is explained by a one-step process with a short core hole lifetime. However, the final state interaction involving the van Hove singularities is not yet fully understood.

In this work, we report the $M_{2,3}VV$ Auger spectral profiles of Cu(110) at excitation energies near the Cu 3p core electron excitation threshold. As the Auger profile of Cu will appear with the multiplet satellite and at binding energies far from the valence band spectral profiles, it is suitable to study the detailed Auger spectral profile based on atomic theory [12, 13]. Since the photoexcited core hole in the 3p level may have a longer lifetime than that in the 2p level and the photoexcitation probability to the valence states may be different between the 2p and 3p core levels, the resonant Auger effect involving the van Hove singularities above E_F is expected to be different from that of the $L_{2,3}VV$ Auger process.

2. Experimental details

Photoemission measurements were carried out at BL4 of the Siam Photon Laboratory of the Synchrotron Light Research Institute (SLRI) [14]. The photoemission system is equipped with an ion gun, an electron gun, low-electron-energy diffraction (LEED) optics, a temperature-controlled sample holder and an electron-energy analyzer (Thermo VG Scientific; CLAM2). The acceptance angle of CLAM2 is 30°, which is sufficient for covering the surface Brillouin zone of Cu in this experiment. Pressure in the analysis chamber was below 2×10^{-10} mbar during photoemission measurements. The overall energy resolution of the measured spectra was 220 meV at an excitation energy of 80 eV, which was confirmed by the energy width of E_F of a gold sample at room temperature.

A clean single-crystal Cu(110) sample was prepared by repeated cycles of argon-ion bombardment and subsequent annealing at 870 K. The amounts of carbon, oxygen and sulfur impurities were monitored by Auger electron spectroscopy (AES), and they were observed to be below the detection limit of AES on the clean Cu(110) surface. The sample surface showed a very sharp and low-background p(1 × 1) LEED pattern.

3. Results and discussion

Figure 1 shows the photoemission spectrum of Cu(110) measured at an excitation energy of 75.5 eV, close to the 3p core electron excitation threshold. In the spectrum, the intense features, ranging from E_F to a binding energy of about 9 eV, correspond to the Cu valence band. The valence band satellites appear in the binding energy range above 10 eV, and they do not overlap with the valence band structure [15, 16]. This suggests that the intra-atomic Coulomb interaction in Cu is much larger than the valence band width of 9 eV. The multiplet calculations for $3d^8$ and $3d^7$ configurations by Robert *et al* [17] and the L_3VV resonant Auger spectrum measured by Föhlisch *et al* [10] are also shown in the figure. As shown in figure 1, the observed spectral features of the satellite are well reproduced by the multiplet terms of the $3d^8$ configuration, while those of the $3d^7$ configuration are not clearly discernible in the spectrum. In the figure, the spectral features of the $3d^8$ satellite are resonantly enhanced near the 3p core electron excitation threshold, and they reveal the $M_{2,3}VV$ Auger decay above it. Our result suggests that the photoexcited 3p core hole decays mainly to the $3d^8$ final state as in the case of the L_3VV Auger profile, and the valence band structure does not appreciably influence the $M_{2,3}VV$ Auger spectral profile. This implies that the intra-atomic Coulomb interaction estimated from the profile is very similar to that in the L_3VV Auger profile on the basis of Cini–Sawatzky theory [12, 13].

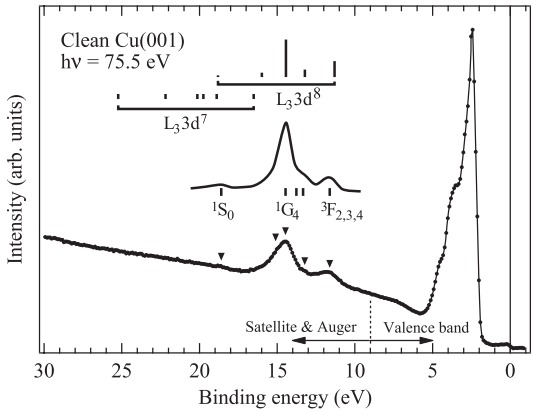

Figure 1. Photoemission spectrum of Cu(110) measured at an excitation energy near the Cu 3p core electron excitation threshold (75.5 eV). The multiplet structures of the L_3VV resonant Auger profile reported by Föhlisch *et al* [10] and theoretical calculation by Roberts *et al* [17] are also shown.

Figure 2 shows the $M_{2,3}VV$ Auger profiles measured at excitation energies between 72 and 86 eV. In the figure, the binding energies of the $^1S_0$, $^1G_4$ and $^3F_{2,3,4}$ multiplet terms in the $3d^8$ satellite are shown by dashed lines. It is obvious in the figure that the intensities of the multiplets are enhanced when they overlap with the $M_{2,3}VV$ Auger profile. Furthermore, the peak positions of the $^1G_4$ and $^3F_{2,3,4}$ terms are shifted to the low binding energy side at the excitation energy of the 3p core electron excitation threshold. To investigate the energy shift of spectral profiles, we have plotted them as a function of kinetic energy. Figure 3 shows the $3d^8$ satellite and the $M_{2,3}VV$ Auger profiles of Cu measured at excitation energies between 74 and 120 eV. The abscissa represents the kinetic energy of the photoelectrons, and the excitation energy is indicated on the right-hand side of each spectrum. In the

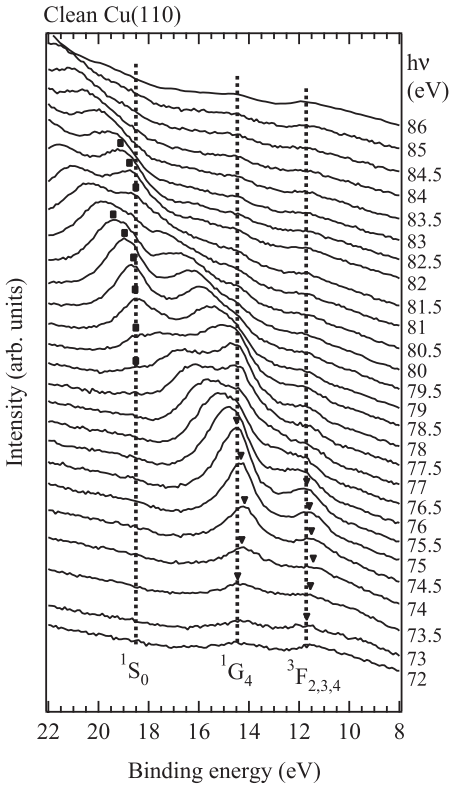

Figure 2. Photoemission spectra of Cu(110) measured in the excitation energy range between 72 and 86 eV. The excitation energy is indicated on the right-hand side of each spectrum. Dashed lines indicate the binding energies of the $^1S_0$, $^1G_4$ and $^3F_{2,3,4}$ multiplet terms in the $3d^8$ satellite. Peak positions of the satellite multiplets are indicated by solid triangles and squares.

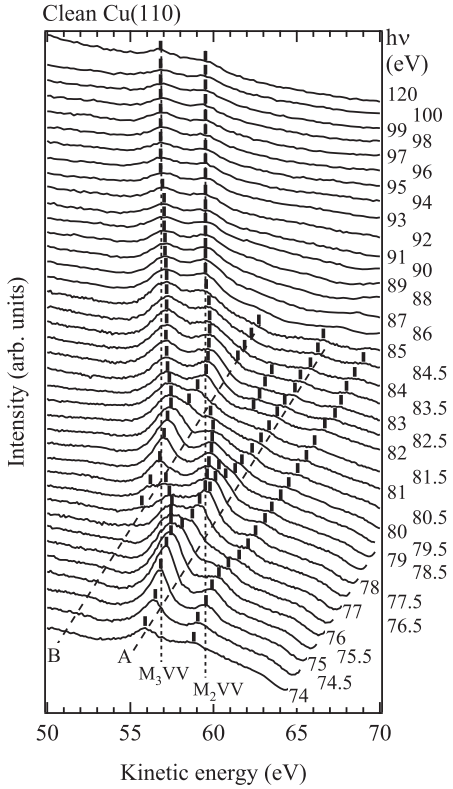

Figure 3. $M_{2,3}VV$ Auger spectra of Cu(110) measured in an excitation energy range between 74 and 120 eV. The abscissa represents the kinetic energy of the photoelectrons and the excitation energy is indicated on the right-hand side of each spectrum. Vertical dashed lines represent the kinetic energies of the normal Auger electrons and ticks represent the peak positions of the satellite and $M_{2,3}VV$ Auger profiles. Dashed lines A and B corresponding to the $^1G_4$ and $^1S_0$ terms in figure 3 are guide lines for the eye.

figure, the dashed lines represent the expected kinetic energies of normal $M_{2,3}VV$ Auger electrons, which are estimated to be 56.8 and 59.4 eV for the M_3VV and M_2VV Auger electrons, respectively, from the averaged spectral profiles observed in the photon energy range between 100 and 120 eV. In this excitation energy range, the Auger profile is interpreted as a normal Auger profile without considering any final state interactions, and the Auger profile is composed of a twofold structure by the M_2 and M_3 excitations, which are separated by a spin–orbit interaction of 2.6 eV. Ticks indicate the peak positions of the satellite and $M_{2,3}VV$ Auger profiles. In the figure, the $M_{2,3}VV$ Auger profiles reveal prominent peaks due to the $^1G_4$ final state at kinetic energies of 56.8 and 59.4 eV for the M_3 and M_2 excitations, respectively, and above the 3p core electron excitation threshold they are shifted to energies greater than that of the normal Auger electrons.

To investigate this kinetic energy shift of the Auger electrons near the 3p core electron excitation threshold, we plotted the photon energy dependence of the peak positions of the Auger profile. In figure 4, the dotted lines correspond to the kinetic energies of the normal Auger electrons, and the dashed lines, designated by letters A and B, correspond to the constant binding energies of the $^1G_4$ and $^1S_0$ terms as 14.5 and 18.5 eV, respectively. The kinetic energies of both the M_2VV and M_3VV Auger electrons decrease with an increase in the excitation energy above the 3p core electron excitation threshold. The deviation from constant kinetic energies of the normal Auger electrons is more obvious in the M_3VV than in the M_2VV Auger electrons. In the M_3VV Auger profile, the shift of the kinetic energy of the $^1G_4$ term spreads over 10 eV from the 3p core electron excitation threshold, which may partly include a weak contribution of the $^3F_{2,3,4}$ term due to the rather small spin–orbit splitting energy of the Cu 3p level. In the figure, we also show the total yield spectrum measured by a sample-drain current. It should be remarked that the total yield spectrum shows kinks at excitation energies corresponding to the M_2 and M_3 excitations at 75.1 and 77.7 eV. The total yield spectrum also shows kinks at the excitation energies from the M_2 and M_3 core levels to the L_1 and X_1 van Hove singularities in the valence states, where the density of valence states shows a maxima above E_F. The energies of the L_1 singularity at 4.2 eV and the X_1 singularity at 7.7 eV above E_F are adopted from reported experimental and calculated data [15, 16].

In Cu, the $3d^8$ satellite is resonantly enhanced due to the interference effect between the direct valence electron excitation ($3p^63d^94s^2 + h\nu \rightarrow 3p^63d^84s^2 + \varepsilon l$) and the 3p core electron excitation followed by the $M_{2,3}VV$ Auger decay, forming a two-hole final state at an atomic site ($3p^63d^{10}4s^1 + h\nu \rightarrow 3p^53d^{10}4s^2 \rightarrow 3p^63d^84s^2 + \varepsilon l$). Near the 3p core electron excitation threshold, the Auger final state combines

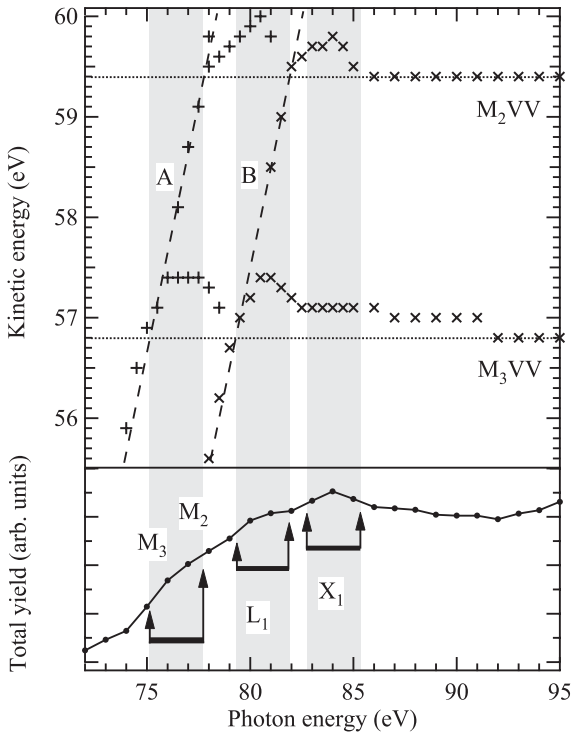

Figure 4. Excitation energy dependence of kinetic energies of $M_{2,3}VV$ Auger electrons and total yield spectrum of Cu(110). Dotted lines correspond to the kinetic energies of the normal Auger electrons, and the dashed lines, designated A and B, correspond to the constant binding energies of the $^1G_4$ and $^1S_0$ terms, respectively. Linked arrows represent the 3p core electron excitation thresholds and the 3p core electron excitations to the L_1 and X_1 van Hove singularities.

with the one-electron state, which is bound by a core hole and localized in a Cu atom. Since the binding energy of this one-electron state by the two holes in the Auger final state is larger than that by the single hole in the final state of the direct photoelectron excitation, the resonantly enhanced satellite electrons show higher kinetic energies than those of the normal Auger electrons. It is reasonable to understand that the hole screening and the delocalization of one- and two-hole states become smaller as the excitation energy increases, because the screening and the delocalization of d holes are less effective by an s-like electron than by a d-like electron excited from the 3p core levels. Therefore, the kinetic energies of the Auger electrons decrease as the excitation energy increases, because the hybridization between Cu 3d states and other valence states is smaller in the higher energy valence states.

In figure 4, the kinetic energies of the $M_{2,3}VV$ Auger electrons do not show an obvious dip structure at the excitation energies to the L_1 and X_1 van Hove singularities in the valence states as previously observed in the $L_{2,3}VV$ Auger electrons [10]. Instead, we observed that the kinetic energies of the $M_{2,3}VV$ Auger electrons decrease to those of the normal Auger electrons with several step features. The differences between the LVV and MVV Auger profiles are simply explained by the lifetime of the excited core hole. Since the 2p core hole has a shorter lifetime, the LVV Auger profile is well described by the one-step model resulting in a resonant profile, while the final state interaction plays a dominant role in the MVV Auger profile caused by the 3p core hole with a longer lifetime.

In figure 4, the positions of the steps correspond to the excitation energies to the L_1 and X_1 van Hove singularities, and the step height is larger for the L_1 point than for the X_1 point. Since the Cu valence states show a large density of unoccupied states at high symmetry points in the Brillouin zone, it is reasonable to consider that the transition probabilities of 3p core electron excitation to the L_1 and X_1 points are larger than those to other valence states. It should also be considered that the localization of the two-hole final state is stronger at the L_1 point than at the X_1 point, since the stronger hybridization between Cu 3d states with other valence states is energetically favored at the L_1 point rather than at the X_1 point. This may cause a large kinetic energy shift of the Auger electrons and hence a larger step height at the excitation energy corresponding to the L_1 point.

In summary, we have observed that in Cu the kinetic energies of the $M_{2,3}VV$ Auger electrons shift to an energy higher than that of the normal Auger electrons and decrease as the excitation energy increases above the Cu 3p core electron excitation threshold. In the excitation energy dependence of the kinetic energies of the $M_{2,3}VV$ Auger electrons, we observed step features at the excitation energies corresponding to the 3p core electron excitations to the L_1 and X_1 van Hove singularities in the unoccupied valence states. The kinetic energy shifts of the $M_{2,3}VV$ Auger electrons are reasonably understood by considering the localization of the two-hole Auger final state and the hybridization between Cu 3d states and other valence states.

Acknowledgments

The authors thank all of the technical staff members of SLRI for their support. One of the authors (AK) thanks Professor Kosugi for valuable discussion. This work is supported by the Thailand Center of Excellence in Physics.

References

[1] Coward D M and Thurgate S M 2000 *J. Electron Spectrosc. Relat. Phenom.* **107** 193
[2] Jach T and Powell C J 1981 *Phys. Rev. Lett.* **46** 953
[3] Iwan M, Himpsel F J and Eastman D E 1979 *Phys. Rev. Lett.* **43** 1829
[4] Davis L C and Feldkamp L A 1979 *J. Appl. Phys.* **50** 1944
Davis L C and Feldkamp L A 1980 *Phys. Rev. Lett.* **44** 673
[5] Parlebas J C, Kotani A and Kanamori J 1982 *J. Phys. Soc. Japan* **51** 124
[6] Drube W, Treusch R and Materlik G 1995 *Phys. Rev. Lett.* **74** 42
Drube W, Grehk T M, Treusch R, Materlik G, Hansen J E and Åberg T 1999 *Phys. Rev.* B **60** 15507
Drube W, Treusch R, Sham T K, Bzowski A and Soldatov A V 1998 *Phys. Rev.* B **58** 6871
[7] Gel'mukhanov F and Ågren H 1999 *Phys. Rep.* **312** 87
[8] Guillot C, Ballu Y, Paigné J, Lecante J, Jain K P, Thiry P, Pinchaux R, Pétroff Y and Falicov L M 1977 *Phys. Rev. Lett.* **39** 1632

[9] Takata Y, Hatsui T and Kosugi N 1999 *J. Electron Spectrosc. Relat. Phenom.* **101–103** 443
[10] Föhlisch A, Karis O, Weinelt M, Hasselström J, Nilsson A and Mårtensson N 2002 *Phys. Rev. Lett.* **88** 027601
[11] Sarma D D, Barman S R, Cimino R, Carbone C, Sen P, Roy A, Chainani A and Gudat W 1993 *Phys. Rev.* B **48** 6822
[12] Cini M 1977 *Solid State Commun.* **24** 681
Cini M 1978 *Phys. Rev.* B **17** 2788
[13] Sawatzky G A 1977 *Phys. Rev. Lett.* **39** 504
Sawatzky G A and Lenselink A 1980 *Phys. Rev.* B **21** 1790
[14] Nakajima H, Buddhakala M, Chumpolkulwong S, Supruangnet R, Kakizaki A and Songsiriritthigul P 2007 *Proc. 9th Int. Conf. on Synchrotron Radiation Instrumentation (Daegu 2006)*; *AIP Conf. Proc.* **879** 543
[15] Courths R and Hüfner S 1984 *Phys. Rep.* **112** 53
[16] Marini A, Onida G and Sole R D 2001 *Phys. Rev. Lett.* **88** 016403
[17] Roberts E D, Weightman P and Johnson C E 1975 *J. Phys. C: Solid State Phys.* **8** L301